DOI: 10.56452/2021SP-8-034

ISSN: 0974-5823 Vol. 6 (Special Issue 4, November 2021)

International Journal of Mechanical Engineering

Comparative Study of $BiFe_{1-X}Zr_XO_3$ (x= 0, 0.1, 0.2) Prepared by Solid State Reaction and Sol-Gel Method

Anamol Gautam[1] and Anshul Jaswal[2]

[1]Department of Applied Science, Chandigarh Engineering College, Jhanjeri-140307, Punjab, India
[2]Department of Computer Application, Department of Applied Science, Chandigarh Engineering College, Jhanjeri-140307, Punjab, India

Abstract: Composition of $BiFe_{1-X}Zr_XO_3$ (X = 0.1, 0.2) were prepared by conventional solid state reaction technique , calcined at 800^OC and sintered at 820^OC. Same composition is synthesized by sol gel method using water soluble inorganic salts at 80^OC for 5 h annealed at 600^OC temperature and sintered at 650^OC in air atmosphere. The crystallite size 24nm and 28nm for x= 0.1 and 0.2 respectively was observed in samples prepared by sol gel method. A dielectric anomaly indicating magnetoelectric coupling is observed in all samples showing relaxor behavior and decrease in T_N with doping is observed.

Keywords: Nanoceramics, multiferroic, magnetoelectric, ferroelectric

Introduction

In recent years, perovskite type multiferroic material $BiFeO_3$ which exhibits coexistence of magnetic and ferroelectric ordering in a certain temperature range, has attracted much attention because of the possible inter relationship between the magnetization and the ferroelectric properties of the materials. This relation is accepted to be basis of a memory device by a combination of ferroelectric and ferromagnetic properties [1-5]. Besides this, there is promising applications in exploiting physics of magnetoelectric materials. It is well accepted that $BiFeO_3$ exhibits antiferromagnetic ordering (T_N = 380ºC) and ferroelectric behavior with high ferroelectric Curie temperature (T_C = 830ºC). To improve the properties of $BiFeO_3$ considerable efforts have been made, for instance, Bi site substitution with Nd^{3+}, Gd^{3+} and Pr^{4+} and Fe site substitution with Ni^{2+}, Cr^{3+}, Ti^{4+} and Nb^{5+}, since the ferroelectricity and magnetism of $BiFeO_3$ come from the lone pair electrons of Bi^{3+} ions and the magnetism of Fe^{3+} ions respectively[6-14]. Classic perovskite type ferroelectric material $Pb(ZrTi)O_3$ is well known to be derived from perovskite type ferroelectric material $PbTiO_3$ through the substitution of Ti with Zr [15]. Substantially enhanced ferroelectric and piezoelectric functional properties are usually thought to arise from the increase from the electric domains mobility on Zr substitution. Moreover, as an antiferroelectric material, $PbZrO_3$ was also extensively studied. A comparative study of Zr doped showed intense polarization motion and an unalterable valence of 4+, the relatively higher valence made it as an acceptor in some compounds [16-18]. Also, considering the fact that the valence of Zr^{4+} ions is higher than the Fe^{3+} and ionic radius of Zr^{4+} (0.072 nm) is larger the that of Fe^{3+}(0.064 nm), it is expected that high valence Zr^{4+} substitution for Fe^{3+} at the B site could fill the oxygen vacancies induced by the possible transition from Fe^{3+} to Fe^{2+} and suppress the inhomogeneous magnetic spin structure to improve the magnetic properties of $BiFeO_3$. Ferroelectric nanoceramics have been considered as a material of great technological importance in the development of high-density storage devices. The microstructure and properties of these nanomaterials depend in an extreme manner on the synthesis method as well as on the processing route and it becomes important to select the most appropriate technique for preparation of these materials with desired properties. Classically, these powders are produced using high temperature mixed oxide method, which eventually proved to be inadequate from the standpoint of chemical homogeneity, purity and uniformity. Although the

problem is overcome by sol–gel method and coprecipitation method [19], the two methods still need high temperature about up to 600°C. Hydrothermal method [20] is also a good way to resolve all the above problems, but it has a long reaction time over 12 h. Hence, despite the intense study, a fundamental understanding of structure property correlations in $BiFeO_3$ is still lacking. Specifically, the nature of magnetic response and the fundamental dependence of dielectric and ferroelectric behavior on the size and precise chemical composition (doping) are issues of great interest. Here we present a comparative study of the synthesis of Zr doped $BiFeO_3$ ceramics synthesized by conventional solid state versus sol-gel synthesized ceramics.

Experimental

$BiFe_{1-X}Zr_XO_3$, ceramic sample was prepared by a conventional solid state reaction technique. Bi_2O_3, Fe_2O_3 and ZrO_2 were used as starting reagents. The ratio of components was taken in accordance with the stoichiometric formula. The calcination of the finely ground powder was done at 800^OC. The pellet specimen of 1 mm thickness and 7 mm diameter were prepared with an organic binder and sintered at 820^OC in air atmosphere. Sintered pellets were polished and flat surfaces were coated with silver paste then dried at 100^OC for 30 min before taking electrical measurements. At the same time sol gel samples with the composition $BiFe_{1-X}Zr_XO_3$ (X = 0.1, 0.2) were prepared using water soluble inorganic salts. Bismuth nitrate $Bi(NO_3)_3{\cdot}5H_2O$, ferric nitrate $Fe(NO_3)_3{\cdot}9H_2O$, zirconium nitrate $Zr(NO_3)_4{\cdot}3H_2O$, citric acid and ethylene glycol were used as starting materials. Appropriate molar proportion of metal nitrates was fixed at Zr:Bi:Fe ratio of 1:9:10, 1:4:5. The precursor solution was dried at 80^OC for 5 h to obtain the $BiFe_{1-X}Zr_XO_3$ xerogel powders. The xerogel initially started to swell and filled the beaker producing a foamy precursor. Then, the xerogel powders were ground and the resulting powders were annealed at 600^OC temperature. The phase purity of the materials was obtained using the XRD of the sintered pellets using Cu Kα radiation at a slow scanning rate of 10/min. The pellet specimen of 1 mm thickness and 7 mm diameter were prepared with an organic binder and sintered at 650^OC in air atmosphere. Sintered pellets were polished and flat surfaces were coated with silver paste and then dried at 100^OC for 30 min before taking electrical measurements. The dielectric constant (ε) and loss tangent (tanδ) of the compounds were measured using an automated HIOKI 3532-50 Hi Tester, LCR meter capacitance measuring assembly in the temperature range 50 – 400 ^OC. The magnetic hysteresis (M-H) loop was measured using a vibrating sample magnetometer (VSM) supplied by Priston Applied Research (155) with a maximum magnetic field of 10kOe.

Results and discussion

X-ray diffraction studies Figure 1 and Figure 2 show the powder XRD patterns of $BiFe_{1-X}Zr_XO_3$ (x= 0, 0.1, 0.2) samples prepared by solid state and sol gel method respectively. It can be seen that the XRD spectra of $BiFe_{1-X}Zr_XO_3$ samples have majority $BiFeO_3$ phase crystallization. However, a small amount of impurities like $Bi_2Fe_4O_9$ were observed. $BiFeO_3$ is a meta stable compound and because of its chemical kinetics of formation it is associated with some impurity phases as $Bi_{25}FeO_{40}$, $Bi_2Fe_4O_9$. XRD patterns show that with the increasing concentration of Zr the peaks shifts to the smaller angle and this suggests that the lattice constant is increased by the Zr substitution, as the radius of Zr^{4+} (0.072 nm) is larger the that of Fe^{3+} (0.064 nm), The lattice parameters are a = b = 5.596Å, c = 13.730 Å, for x = 0.1 and a = b = 5.605Å, c = 13.647 Å, for x = 0.2 prepared by solid state method. The lattice parameters (equivalent hexagonal) for $BiFe_{1-X}Zr_XO_3$ are: a = 5.596 Å, c = 13.787 Å and a = 5.597 Å, c = 13.695 Å respectively for x = 0.1 and x = 0.2 prepared by sol gel method.

DOI: 10.56452/2021SP-8-034

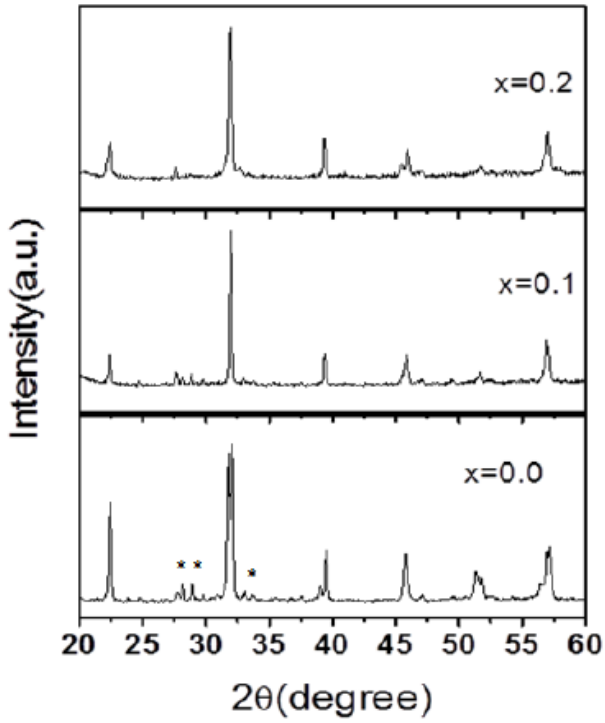

Figure 1 X-ray diffraction pattern for BiFe1-xZrxO3, system (x = 0.0, 0.1, 0.2 and 0.3) prepared by solid state method, (*) represents the $Bi_2Fe_4O_9$ impurity phase.

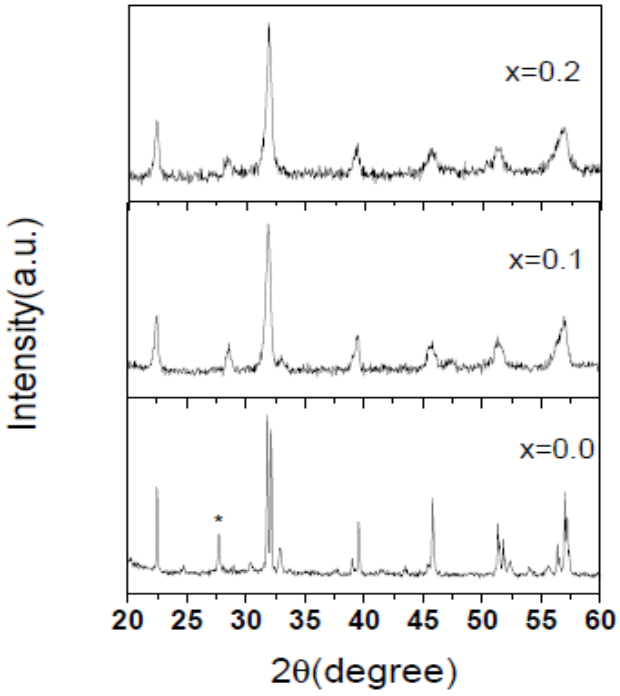

Figure 2 X-ray diffraction pattern for $BiFe_{1-X}Zr_XO_3$, system (x = 0.0, 0.1, 0.2) prepared by sol gel method, (*) represents the $Bi_2Fe_4O_9$ impurity phase.

The use of the amorphous citrate process has the advantage that the homogeneity of an aqueous solution of salts is preserved in a gel medium and possibly the final product, enabling effective substitution into $BiFeO_3$ with homogeneity. All the reflections in the XRD pattern of sol gel (Figure 2) are broad due to the nanocrystalline nature of the sample synthesized at low temperatures. The average crystallite size is calculated

from x-ray line broadening using the Scherrer formula, $D = k\lambda/\beta\cos\theta$, where D is the crystallite size in Å, k is shape factor, β is the half maximum line width corrected for instrumental line broadening, and λ is the wavelength of x rays. The crystallite size is obtained as 24nm and 28nm for x= 0.1 and 0.2 respectively.

Microstructural properties SEM photograph (Figure 3) reveals that the microstructure of the samples prepared by solid state method is uniform. The grain growth is homogeneous and randomly oriented. The average grain size was found to be of the order of ~1-2 μm and no segregation of Zr at grain boundaries was observed in SEM. Figure 4 exhibits a SEM microstructural image of samples prepared by sol gel method, which was crystallized at 600 ^{O}C. It is clear that the grains exhibits a uniform feature with approximately 200 nm in size, which is smaller than $BiFeO_3$ powder prepared by the usual solid state reaction method [11]. It demonstrates that sol–gel process is a good method for preparing nanoparticles with uniform features. Sol–gel derived fine powders are usually more homogeneous and reactive due to atomic level mixing than those prepared by conventional solid-state reaction

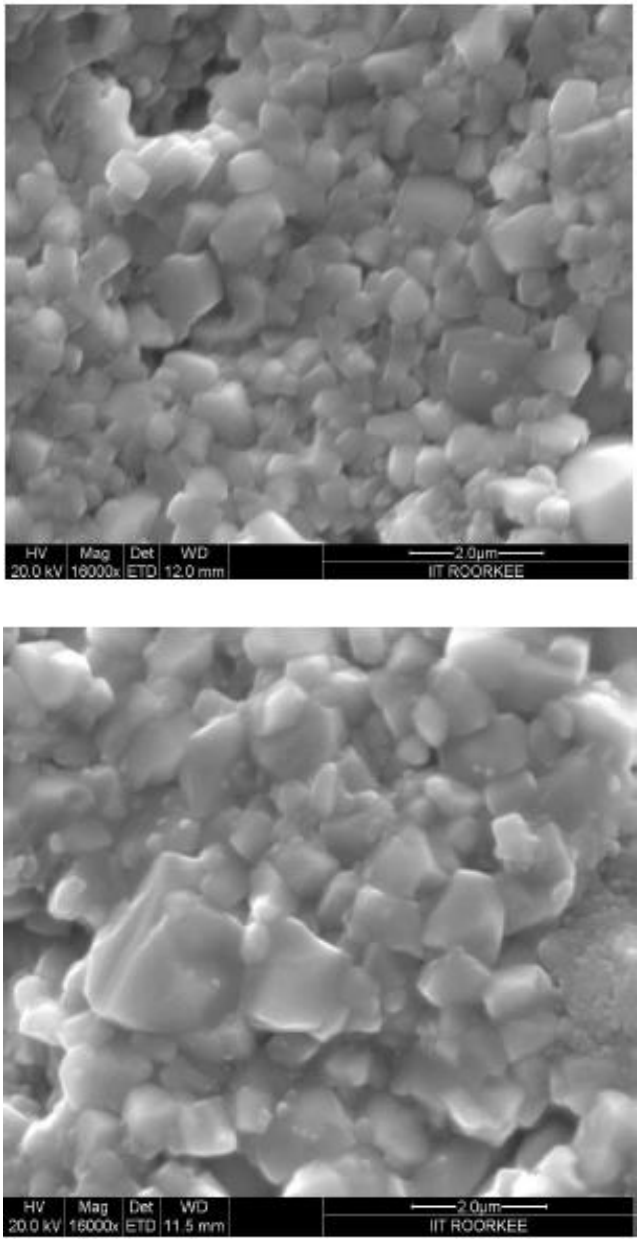

Figure 3 FESEM images of $BiFe_{1-X}Zr_XO_3$ (x = 0.1 & 0.2) ceramics.

DOI: 10.56452/2021SP-8-034

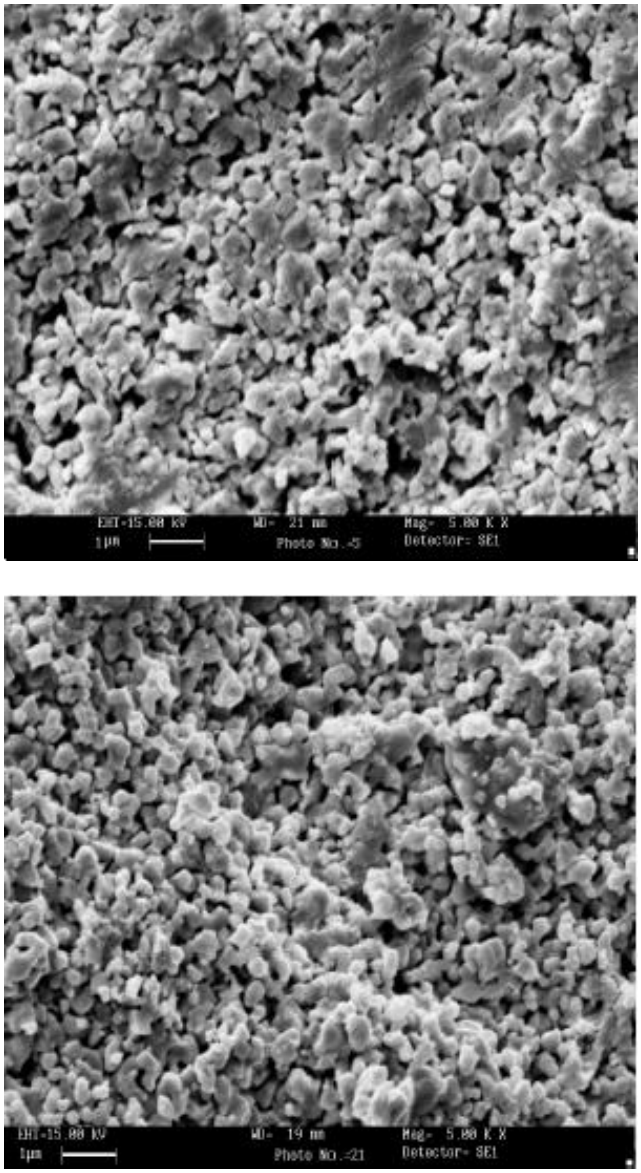

Figure 4 FESEM images of $BiFe_{1-X}Zr_XO_3$ (x = 0.1 & 0.2) nanoceramics.

Dielectric properties Figure 6 and Figure 6 presents the temperature variation of dielectric constant at three different frequencies ranging from 1kHz, 10kHz and 1MHz for $BiFe_{1-X}Zr_XO_3$ samples prepared by solid state reaction method and nanoceramics respectively.

DOI: 10.56452/2021SP-8-034

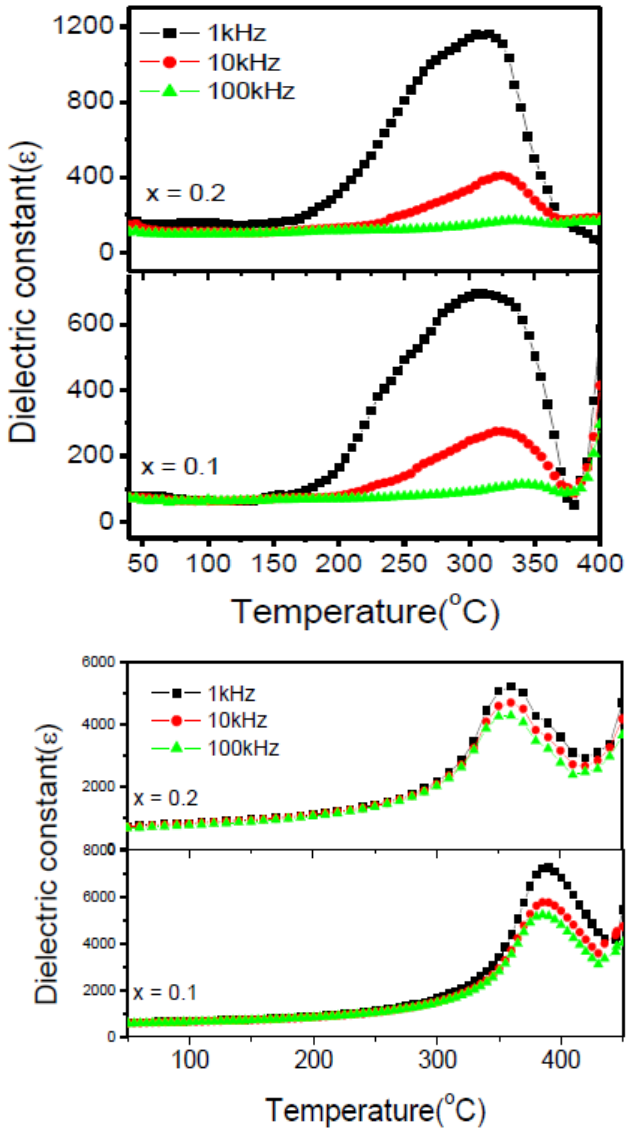

Figure 5 & 6 Dielectric constant vs. temperature plot for $BiFe_{1-X}Zr_XO_3$ (x =0.1, 0.2) samples prepared by solid state method and sol gel nanoceramics.

A dielectric anomaly in the dielectric constant has been observed for all the compositions, indicating magnetoelectric coupling. The peaks in the permittivity patterns and sharp increase in the dielectric constant obtained here may be attributed to change from one state of electric dipole ordering to another because of antiferromagnetic transitions or a possible magnetoelectric coupling effect. The anomaly in the permittivity pattern frequency dependent just as a normal relaxor. The Maxwell-Wagner component arises from grain boundary interfaces in these polycrystalline samples as well as from intrinsic heterogeneity which give rise to broad magnetic transition around ~330 ^OC which is close to T_N .

Similarly the samples prepared by sol gel method show an anomaly at antiferomagnetic transition. But the transition is sharp as compared to that of samples prepared by solid state method. Smaller grain size could be a reason for this behavior. The T_N values decrease from 380 ^OC for x = 0.1 to 360 ^OC for x = 0.2.

Magnetic properties

Figure 7 shows the magnetization hysteresis (M-H) loops of $BiFe_{1-X}Zr_XO_3$ (x=0.1–0.2) samples for the maximum magnetic field of 10 kOe. It is evident that the antiferromagnetism intrinsic in $BiFeO_3$ becomes weak ferromagnetism with a small but non zero M_r of 0.004 emu/g (x = 0.1) and 0.0109 emu/g (x = 0.2) in

BiFe1-xZrxO3. The continuing increase in M_r in our samples is likely due to the continuing collapse of the space-modulated spin structure.

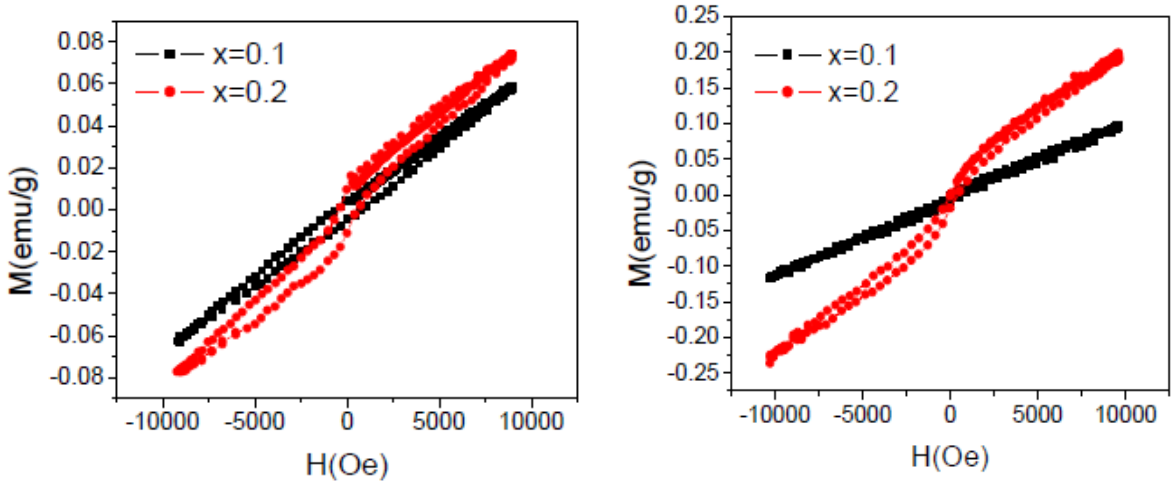

Figure 7 & 8 Room temperature magnetic hysteresis plots for $BiFe_{1-x}Zr_xO_3$ (x = 0.1, 0.2) ceramics and nanoceramics.

As known to us, there is no magnetic interaction between Zr^{4+} and Fe^{3+} since Zr^{4+} is nonmagnetic, but a small amount of Zr^{4+} doping at Fe-site of $BiFeO_3$ perturbs the superexchange interaction Fe–O–Fe because of change in Fe–O–Fe angle and Fe–O distances by Zr^{4+} doping. As the superexchange interaction is sensitive to bond angles and bond distances, the spiral spin structure might be destroyed completely by doping of Zr^{4+} which leads to the release of latent magnetization and the enhancement of remanent magnetization.

The nanoceramics also show similar trend that Mr increases with increase in Zr content (0.011emu/g for x = 0.1 and 0.019emu/g for x = 0.2), But the magnetization is doubled in nanoceramics because of smaller grain size. Magnetic response observed as a function of the applied magnetic field increases with decreasing the particle size.

Conclusion

Prepared Zr doped $BiFeO_3$ ceramics via solid state method as well as sol-gel method and investigated the effect of doped ions on the structural, dielectric and magnetic properties and find that sol–gel process is a good method for preparing nanoscale $BiFe_{1-x}Zr_xO_3$ particles with uniform features. Sol–gel derived fine powders are usually more homogeneous sand reactive due to atomic level mixing than those prepared by conventional solid-state reaction. The value of transition temperature T_N decreases with increase of Zr concentration for both nanoceramics and samples prepared by Solid state method.

References

1. R Ramesh and N A Spladin, “Multiferroics:progress and prospects in thin films”, Nature mater., 6, 21 (2007)
2. B Ramachandran and M S R Rao, “Low temperature magnetocalorific effect in polycrystalline $BiFeO_3$ ceramics”, Appl. Phys. Lett, 95, 142505 (2009).
3. Z G Mei, S L Shang, Y Wang and Z K Liu, “Thermodynamics of multiferroic $BiFeO_3$: Applications for the deposition of $BiFeO_3$ thin films”, Appl. Phys. Lett., 98, 131904 (2011).
4. Y Tokura, “Multiferroics as Quantum electromagnets”, Science, 312, 1481 (2006).
5. G Catalan and J F Scott, “Physics and applications of Bismuth ferrite”, Adv.Mater., 21, 2463 (2009).

6. I N Leontyev, Y I Yuzyuk, P E Janolin, M El-Marssi, D Chernyshov, V Dmitriev, Y L Golovko, V M Mukhortov, B Dkhil, "Orthorhombic polar Nddoped $BiFeO_3$ thin film on MgO substrate", Phys Condens. Mater., 23, 332201 (2011).
7. B Yu, M Li, Z Hu, L Pei, D Guo, X Zhao, and S Dong, "Enhanced multiferroic properties of the high-valence Pr doped $BiFeO_3$ thin film", Apll.Phys. Lett., 93, 182909 (2009)
8. R Rai, I Bdikin, M A Valente and A L Kholkin, "Ferroelectric and ferromagnetic properties of Gd-doped $BiFeO_3$–BaTiO3 solid solution", Mater. Chem. Phys., 119, 539 (2010).
9. S K Pradhan, J Das, P P Rout, S K Das, D K Mishra, D R Sahu, A K Pradhan, V V Srinivasu, B B Nayak, S Verma and B K Roul, "Defect driven multiferroicity in Gd doped $BiFeO_3$ at room temperature", J. Magn. Magn. Matter., 32, 3614 (2010).
10. P Kharel, S Talebi, B Ramachandran, A Dixit, V M Naik, M B Sahana, C Sudakar, R Naik, M S R Rao and G Lawes, "Structural, magnetic, and electrical studies on polycrystalline transition- metal-doped $BiFeO_3$ thin films", J. Phys.: Condens. Mater., 21, 036001 (2009).
11. L Hongri and S Yuxia, "Substantially enhanced ferroelectricity in Ti doped $BiFeO_3$ films", J. Phys. D: Appl. Phys., 40, 7530 (2007).
12. F Chang, N Zhang , F Yang , S Wang and G Song, "Effect of Cr substitution on the structure and electrical properties of $BiFeO_3$ ceramics", J. Phys. D: Appl. Phys., 40, 7799 (2007).
13. J K Kim, S S Kim, W J Kim, A S. Bhalla, and R Guo, "Enhanced ferroelectric properties of Cr-doped $BiFeO_3$ thin films grown by chemical solution deposition", Appl. Phys. Lett., 88, 132901 (2006).
14. C. Ostos, O. Raymond, N. Suarez-Almodovar, D. Bueno-Baqués, L. Mestres and J. M. Siqueiros, "Highly textured Sr, Nb co-doped $BiFeO_3$ thin films grown on SrRuO3/Si substrates by rf- sputtering", J. Appl. Phys., 110, 024114 (2011).
15. B H Yang, T G Qiang, M H Yan and X Ao, " Co-precipitation synthesis of $BiFeO_3$ powders", Adv. Mater. Res., 105, 286 (2010). 1
6. Y Wang, G Xu, Z Ren, X Wei, W Weng, P Du, G Shen and G Han, "MineralizerAssisted hydrothermal synthesis and characterization of $BiFeO_3$ Nanoparticles", J. Am. Ceram. Soc., 90, 2615 (2007).
17. J T Han, Y H Huang, X J Wu, C L Wu, W Wei, B Peng, W Huang, and J B Goodenough "Tunable Synthesis of Bismuth Ferrites with Various Morphologies", Adv. Mater. 18, 2145 (2006).
18. I Sosnowska, W Schafer, W Kockelmann, K H Andersen and I O Troyanchuk, "Crystal structure and spiral magnetic ordering of $BiFeO_3$ doped with maganese", Appl. Phys. A, 74, S1040 (2002).
19. N S Gajbhiye, P K Pandey and P Smitha, "Low temperature synthesis of nanostructured PZT for dielectric studies", Synthesis and reactivity in inorganic, metal organic, and nano metal chemistry, 37, 431(2007).
20. R Ranjan, R Kumar and R N P Choudhary, "Effect of Sm substitution on structural, dielectric and transport properties of PZT ceramics", Mater. Chem and Phys, 115, 473 (2009) 21. S A Mabud, "The morphotropic phase boundary in PZT solid solutions", J Appl. Cryst, 13-3, 211 (1980). 22. T J Park, P C Georgia, V J Arthur, M R Arnold and W S Stanislaus, " Size dependent magnetic properties of single-crystalline multiferroic BiFeO3 nanoparticle", Nano Lett., 7, 766 (2007).